Surface Micromachined Turbines

Chia-Lun Tsai and Albert K. Henning
Thayer School of Engineering, Dartmouth College, Hanover, NH 03755-8000

Summary

This paper reports the fabrication of three-dimensional microturbines, free from post-processing assembly, using surface micromachining technology. The fabrication process consists primarily of surface micromachining technology, with a bulk micromachining step to create the turbine flow channel normal to the wafer surface. Stress engineering of microstructures (SEMS), utilizing the stress between near-zero-stress polysilicon and high-stress silicon nitride films, was used to devise the structures. Release of the micro-turbines is accomplished through the bottom surface opening, since turbine vanes contain no release holes. The bending force in the turbine vanes simultaneously prevents stiction to the substrate, and allows the vanes to self-form their final shape. Stators, similar to those found in surface micromachined motors, allow electrical sensing or actuation of fluid flow.

Keywords: Micro-turbines; Stress engineering; Polysilicon; Silicon nitride; Micro-fluidics

Introduction

LIGA [1,2] and bulk micromachined [3,4] microturbines have been investigated previously. In addition, micro-motors exhibiting speeds ranging from tens to hundreds of thousand of rpm have been achieved [5-9]. However, the use of surface micromachining technology to fabricate three-dimensional, integrated microstructures such as micro-turbines, free from post-processing assembly, has been a challange [10].

Earlier, we presented results related to cantilever SEMS (Stress-Engineered Micro-Structures) [11]. In that work, we described a means to create self constructed, out-of-plane micro-structures by engineering the stress between thin films of polysilicon and silicon nitride. Composite LPCVD silicon nitride/polysilicon beams, with wide ranges of thin film thickness ratio were fabricated to study that concept. We demonstrated large out-of-plane deflections (Figure 1) using near-zero-stress polysilicon, and high-stress silicon nitride. We compared the results to prevailing models [12]. Deviations were noted as the nitride thickness became small compared to the polysilicon thickness. To account for them, we proposed a modified formula which agrees closely with our measurements.

We base our present work on the success of those results. We have designed, modeled, and fabricated other SEMS devices, in particular the microturbines reported here. Their fabrication was executed using the facilities of the Microsystems Technology Laboratories at MIT, and the Solid State Microstructures Laboratory at Dartmouth College. This paper describes the fabrication sequence, and demonstrates the microturbine structures thus created.

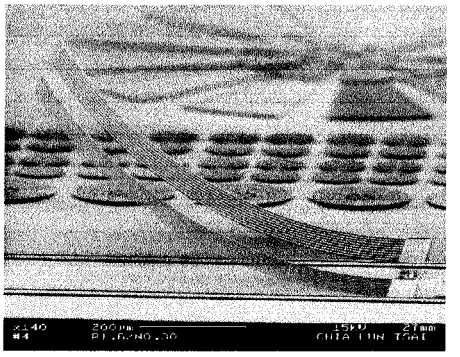

Figure 1: Out-of-plane microstructures (SEMS) based on low-stress polysilicon and high-stress nitride, thin-film sandwiches. Cantilevers such as these were used to model quantitatively the stresses in these structural materials [11].

Fabrication sequence and Mask Design

The fabrication process is shown in Figure 2. Our current micro-turbine fabrication process requires nine mask levels, detailed as follows:

- Step 1. The process begin with 380 μm thick, double-side polished, <100>-oriented silicon wafers. The supporting bridge structures are made by creating a heavily doped boron layer. One side of a double-side polished wafer is heavily doped with boron (>10^{20} cm^{-3}), using solid source, high temperature thermal diffusion, to form an 11 μm thick p+ layer. The areas which will become flow paths normal to the wafer surface are undoped, and protected by 1 μm thick low temperature oxide patterns during this diffusion process. Supporting bridges and flow paths are created using selective KOH etching in step 10. Wafers are cleaned with buffered HF to remove the oxide mask patterns.

- Step 2. The wafers are passivated with 3000 Å stress release thermal oxide, and 1500 Å nitride. A 2 μm LTO layer was deposited as sacrificial layer.
- Step 3. Dimple etch is performed with wet isotropic buffered HF etch for 1 μm in depth to reduce the contact area between the turbine and substrate. The wafers are then cleaned, and patterned with resist for the electrode anchor etch.
- Step 4. LPCVD polysilicon films (1.6, 2.0 and 3.6 μm) were deposited at 580 °C and then annealed at 1050°C for one hour. To maintain a smoother surface and reduce the string effect during plasma etch, we delayed the polysilicon etch until after nitride formation and patterning.
- Step 5. 1500 Å LTO oxide is deposited and patterned to create contact windows for the nitride layer. This oxide layer also serves as the etch stop layer during nitride patterning to protect the polysilicon layer underneath.
- Step 6. LPCVD nitride depositions (1500 Å, 3000 Å, 4500 Å and 7500 Å), patterned anisotropically with plasma etch.
- Step 7. 0.5 μm of LTO (hard mask layer) was deposited and patterned. We then use a Cl_2/HBr plasma etch, which we developed at MIT, to etch the 1.6 to 3.6 μm-thick polysilicon layer with very high quality anisotropic etch profile, to create the turbines and electrodes.
- Step 8. 1μm LTO was deposited as bearing clearance. Anchor etch was performed for the next hub formation.
- Step 9. Hub formation was done by depositing a 1500 Å LPCVD silicon nitride layer, plus a 1 μm LPCVD polysilicon layer at 620 °C. The layers were patterned with Cl_2/HBr and CF_4/CHF_3/Ar plasma etch.
- Step 10. Flow path formation: The front side of the wafer was protected with resist. The backside was patterned using two-sided alignment with 2 μm alignment accuracy, and plasma etched to clean all exposed films and the silicon substrate. After removing the photoresist with an O_2 plasma, a one-sided KOH etch was performed, using carnauba wax to protect the top-side devices. During the KOH etch, airways for micro-turbines were opened, and the supporting bridges which have high boron concentration were also formed, using the high etch selectivity ratio between undoped and doped p-type silicon. The etch is stopped at the nitride layer below the turbine and the sacrificial LTO layer. The carnauba wax is later stripped, and the wafers are cleaned with a standard piranha solution. The front side of wafer is protected again with photoresist, and the wafer backside is exposed to a plasma etch, which

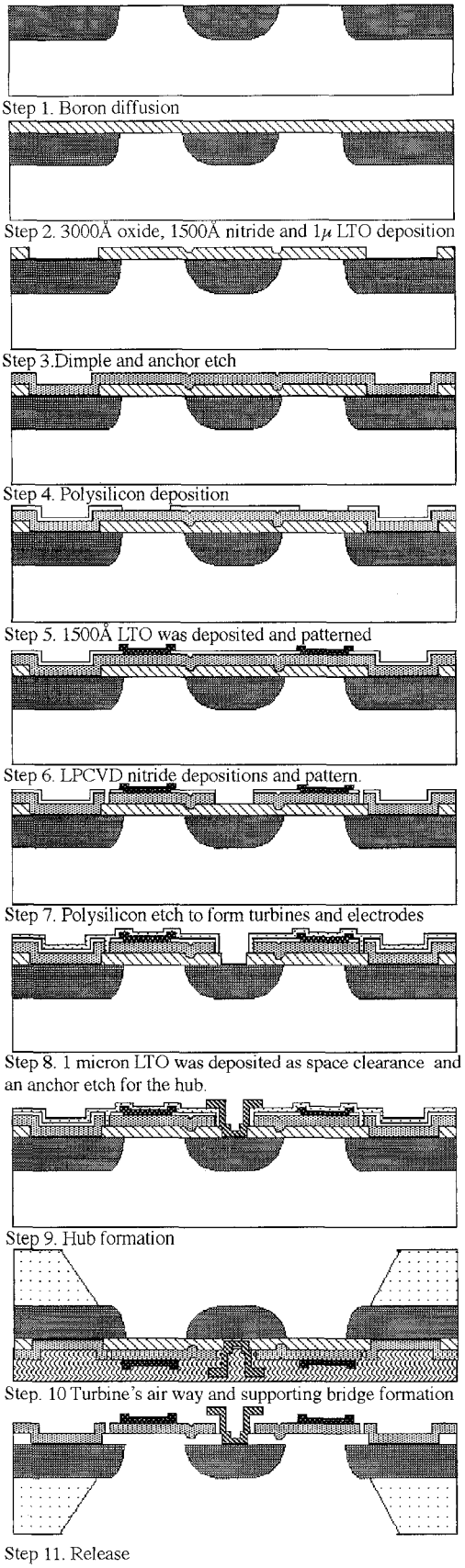

Figure 2: Micro-turbine fabrication sequence

removes the KOH etch stop nitride layer. Figure 3 shows an SEM micrograph of the bridge and flow path, with the micro-turbine vanes removed.

- Step 11. There are no release holes in our turbines; the micro-turbines are mainly released from the back opening. To release the turbine structures mechanically from the substrate, they were cleaned, dipped into buffered HF for ten to fifteen minutes, rinsed with DI water, given a final rinse in isopropyl alcohol, and dried on a hot plate. When releasing the micro-turbines, the bending force must be great enough to prevent stiction to the substrate. All of the devices, regardless of size, were released successfully.

Based on our SEMS modeling work [11], we used the material properties of our low-stress polysilicon and high-stress nitride films to design the micro-turbines. A mechanical modeling tool (ANSYS) supported this effort. The result was a set of masks which explored micro-turbines with a variety of diameters, number of vanes, and nitride structures to create the out-of-plane structure necessary to curve the vanes upon release. A sample micro-turbine design from this mask set is shown in Figure 4. In a qualitative sense, most of the vane curvature in the micro-turbine is induced along the long axis of the nitride stripes, as seen in the next section.

Results and Conclusions

Figures 5 and 6 demonstrate some of our successfully released micro-turbines. Figure 5 shows an eight-vaned turbine rotor. Each vane has six nitride stripes, which create its final out-of-plane structure. The polysilicon and nitride thicknesses are, respectively, 1.6 μm and 4500Å. Figure 6 shows another example; here, there are four vanes, with only two nitride stripes per vane to create the vane curvature. The polysilicon and nitride thicknesses are, respectively, 2.0 μm and 4500Å. In each of these SEM pictures, note the absence of curvature along the radial axis. This feature is essential in creating rotors which not only turn under fluid actuation, but maintain electrostatic contact with the polysilicon stators (also visible in the SEMs), so that the motion can be sensed. Alternatively, of course, the rotors can be actuated electrostatically, in order to create fluid motion.

We have performed some initial tests of the mechanical behavior of these micro-turbines. The tests consisted of directing a continuous flow of nitrogen gas at the surface of the micro-turbine. The mechanical response was observed using a

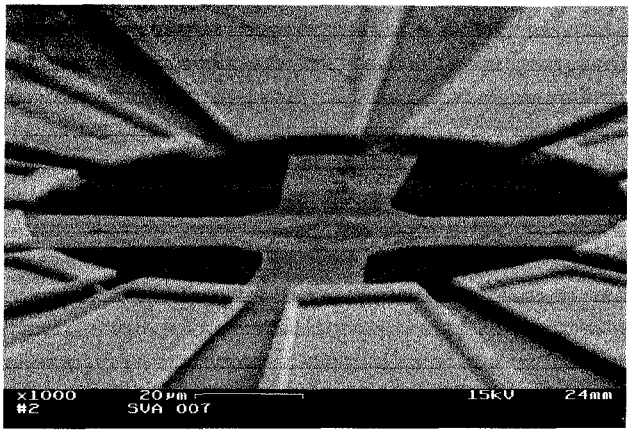

Figure 3: SEM of p+ bridge structure and flow paths in the micro-turbines.

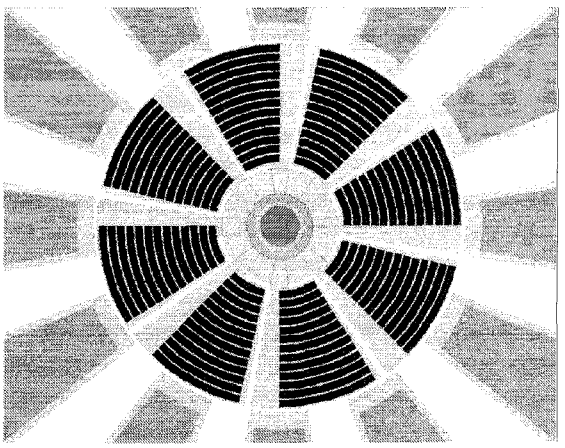

Figure 4: Mask layout of a micro-turbine. Note the curved nitride stripes atop the polysilicon vanes. The shape of these stripes, combined with the stress differences between the polysilicon and nitride layers, gives rise to the final shape of the micro-turbine vanes.

CCD camera. The micro-turbines operated successfully throughout these initial observations. Of course, the application of excess flow can break the turbine blades from the rotor hub. Further experiments to quantify performance of the turbines are underway.

In conclusion, we have successfully demonstrated the design and fabrication of three-dimensional micro-turbine structures. These structures are based on our previously-developed SEMS techniques, utilizing the stresses between thin films of low-stress polysilicon and high-stress nitride to create out-of-plane microstructures. The micro-turbine rotors are supported by boron-doped silicon bridges. Flow paths are created using both surface and bulk micromachining techniques. The turbines are self-formed during the final release process. This backside release process proved essential in creating stiction-free micro-turbines.

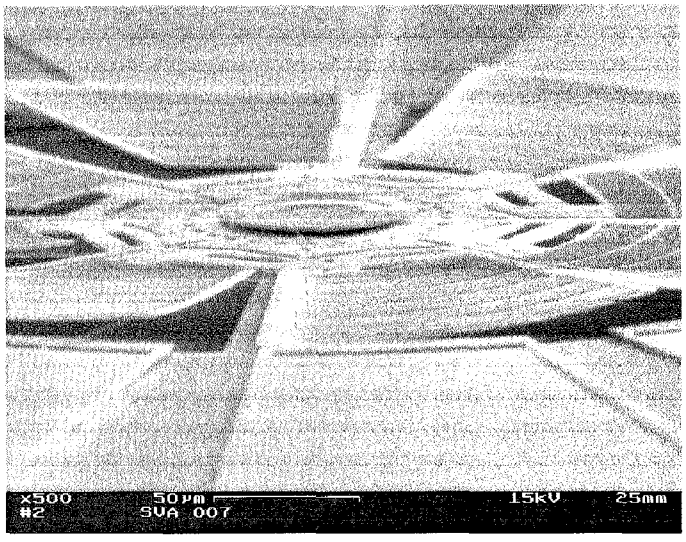

Figure 5: Released micro-turbine. There are eight vanes, and each vane has six nitride stripes used to obtain the curvature shown.

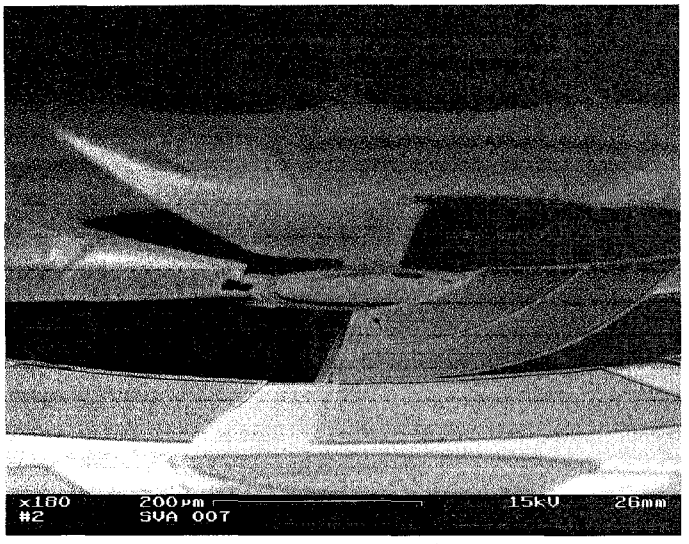

Figure 6: Released micro-turbine. There are four vanes, and each vane has two wide nitride stripes used to obtain the curvature shown.

Acknowledgements

This work has been supported by Analog Devices, Inc., and the Thayer School of Engineering at Dartmouth College. The assistance of the faculty, staff, and students at the Microsystems Technology Lab at MIT is gratefully acknowledged. The authors thank R. Faeth and D. Hopkins of Redwood Microsystems, for the suggestion of the carnauba wax protection process.

References

[1] J. Mohr, P. Bley, C. Burbaum, W. Menz, and U. Wallrabe, "Fabrication of microsensor and microactuator elements by the LIGA process." In Proceedings, *Transducers '91* (IEEE, Piscataway, NJ, 1991), pp. 607-609

[2] M. Himmelhaus, P. Bley, J. Mohr, and U. Wallrabe, "Integrated measuring system for the detection of the revolutions of LIGA microturbines in view of a volumetric flow sensor." *J. Micromech. and Microengg.* **2**, pp. 196-198 (1992)

[3] A. Benitez, J. Esteve, and J. Bausells, "Bulk silicon microelectromechanical devices fabricated from commercial bonded and etched-back silicon-on-insulator substrates." *Sensors and Actuators* **A50**, pp. 99-103 (1995)

[4] D. Mathieson, et al., "Micro torque measurements for a prototype turbine." *J. Micromech. and Microengg.* **4**, pp. 129-139 (1994)

[5] E. J. Garcia, J. J. Sniegowski,"Surface micromachined microengine," *Sensors and Actuators* **A48**, pp. 203-214 (1995)

[6] H. Guckel, T. R. Christenson, K. J. Skrobis, T. S. Jung, J. Klein, K. V. Hartojo, and I. Widjaja, "A first functional current excited planar rotational magnetic micromotor," In Proceedings, *IEEE Micro Electro Mechanical Systems*, (IEEE, Piscataway, NJ, 1993), pp. 7-11.

[7] S. F. Bart, M. Mehregany, L. S. Tavrow, J. H. Lang, and S. D. Senturia, "Electric micromotor dynamics," *IEEE Trans. Elec. Dev.* **ED-39**, pp.566-575 (1992)

[8] L. S. Tavrow. S. F. Bart, and J. H. Lang, "Operational characteristics of microfabricated electric motors," *Sensors and Actuators* **A35**, pp. 33-44 (1992)

[9] D. Mathiesont, B. J. Robertsont, U. Beerschwingert, S. J. Yangt, "Microtorque measurements for a prototype turbine," *J. Micromech. and Microengg.* **4**, pp. 129-139 (1994)

[10] Leslie Ann Field, "Fluid-actuated micromachined rotors and gears." Ph.D. dissertation, UC Berkeley (1991), p. 64.

[11] C.-L. Tsai and A. K. Henning, "Out-of-plane microstructures using stress engineering of thin films." In Proceedings, *Microlith. and Metrology in Micromachining* (SPIE, Bellingham, WA, 1995; K. W. Markus, ed.), volume 2639, pp. 124-132. Also, C.-L. Tsai and A. K. Henning, "Out-of-plane microstructures fabricated using stress engineering," to appear in *J. Vac. Sci. Tech. B.*

[12] M. W. Judy, Y.-H. Cho, R. T. Howe, and A. P. Pisano, "Self-adjusting microstructures (SAMS)," In Proceedings, *IEEE Micro Electro Mechanical Systems* (IEEE, Piscataway, NJ, 1991), pp. 51-56.